# Thermophysical and Thermomechanical Properties of Norland Optical Adhesives and Liquid Crystal Composites

**Réda Benmouna, Boumediène Benyoucef**

*Department of Physics, Research Unit ''Materials and Renewable Energies,'' University Aboubekr Belkaïd, Faculty of Sciences, Tlemcen BP119, Algeria*

Received 15 October 2007; accepted 29 December 2007
DOI 10.1002/app.28039
Published online 19 March 2008 in Wiley InterScience (www.interscience.wiley.com).

**ABSTRACT:** Thermophysical and thermomechanical properties of UV-cured Norland Optical Adhesives (NOA65) and low molecular weight Liquid Crystal E7 systems were investigated. Thin films of Polymer Dispersed Liquid Crystal were prepared by Polymerization Induced Phase Separation and UV-curing. Phase diagrams were established using Polarized Optical Microscopy and DSC to determine the lines of nematic to isotropic phase transition as well as the glass transition temperature changes with the system composition. Mechanical measurements were performed in the static and dynamic modes to determine the moduli in terms of the curing time, the temperature and the amount of low molecular weight liquid crystal molecules. Thermomechanical measurements were found to overestimate the glass transition temperature as compared to calorimetric data. Variations of the Young's modulus and the molecular weight defining the mesh size of the network were analyzed in terms of the curing time and liquid crystal concentration. © 2008 Wiley Periodicals, Inc. J Appl Polym Sci 108: 4072–4079, 2008

**Key words:** glass transition; mechanical properties; rubber; liquid crystal; NOA65

## INTRODUCTION

This article reports on an experimental investigation of thermophysical and thermomechanical properties of Polymer Dispersed Liquid Crystals (PDLCs) elaborated according to the method of Polymerization Induced Phase Separation (PIPS) under photo-curing of a mixture of Norland Optical Adhesives (NOA65) and the low molecular weight liquid crystal E7.[1–5] The exact composition of NOA65 is protected by a commercial patent but it is known in the literature[6,7] that this product is made of thiol-ene molecules containing the $SH_2$— group and multifunctional groups insuring cross-linking and network formation in addition to a photoinitiator. This product is widely used as an efficient non toxic adhesive and in research as a network forming system with a high cross-linking density under UV-irradiation. The liquid crystal E7 is an eutectic mixture for a given composition (see the experimental section). It is characterized by a nematic to isotropic transition at 60°C and a glass transition at −60°C. Therefore, it provides a wide range of temperature for applications under standard conditions (ambient temperature and pressure). Moreover, it has relatively large optical and dielectric positive anisotropies for uses in display devices and commutable windows. Both NOA65 and E7 are available in the market and relatively sheep. More details on these products are given in the Experimental section.

The PDLC composite materials consist of LC micrometric inclusions dispersed in a solid polymer matrix exhibiting a swiss cheese morphology. The interest in these systems resides in their specific electro-optical responses that open up new possibilities for applications in optical fibers, optical shutters, switchable windows, display devices, telecommunication systems and many other developing technologies. For example, current Liquid Crystal Display systems (LCD) function with twisted nematics and require polarizers and surface alignments. The use of the PDLC technology presents the advantage of not necessitating those devices that could absorb a large amount of intensity and reduce their efficiency. In the normal mode operation, films presenting micron-sized droplets are opaque since they produce a strong scattering of visible light in the quiescent state.[8] When activated with an electric field, changes of indices of refraction take place. These in turn result into major changes in the optical properties of the polymerized films that become transparent. Important consequences of these peculiar electro-optic responses were found in the

*Correspondence to:* R. Benmouna (redabenmouna@yahoo.com).

performance of PDLC systems under practical conditions. By tuning the amplitude and frequency of the applied electric field, one could achieve a spectral selectivity of the transmitted light which is useful for telecommunication devices and optical fibers.[9,10]

As mentioned above, the formulation of Norland Optical Adhesives (NOA) contains thiol radicals with the advantage of thiol-ene chemistry since the polymerization is not inhibited by oxygen of the atmosphere like in the case of unsaturated polyesters or acrylates. Bella et al.[11,12] used this formulation together with E7 to analyze the effects of exposure time on the morphology and its development from initial to final states of film formation. They also examined the electro-optic response of these systems by monitoring the transmission of light against voltage during curing process with different UV-source intensities.

Few years later, Lucchetta et al.[13] reexamined similar properties with the same system showing that the use of different exposure times induced large effects outside the illuminated region of the sample because of a substantial diffusion of heat. They demonstrated that the mechanism of phase transition observed was a combination of spinodal decomposition, nucleation and growth.

Sansone et al.[14] considered similar systems (NOA60/E7) and suggested a method for obtaining transparent films exhibiting LC droplets with a size much less than the wavelength of visible light. These films scattered light extremely weakly but showed strong Kerr effects. In a series of papers,[15–18] Kyu and coworkers investigated both experimentally and theoretically the morphology development of photocured NOA65 and the single component nematic liquid crystal K21. Our observations in this work were similar to theirs as far as thermophysical properties were concerned.

Lovinger et al.[19] also reported a detailed study of the morphology and texture of UV-curable PDLCs made of NOA65/E7 formulation. They focussed more on the influence of the radiation dose, curing temperature and initial mixture composition. Qian et al.[20] presented a method of elaboration of a special type of PDLCs which they called Phase Separated Composite Films (PSCF) using NOA65/E7 systems. Their experimental investigation and theoretical analysis showed formation of a dense polymer network at the surface exposed to the radiation while in the interior of the film, a pure LC phase was observed.

Although the properties of NOA and E7 systems were the subject of a particular attention via these references and others,[6,21] to our knowledge no systematic and combined correlative studies of thermophysical and thermomechanical properties were reported so far. The present work is a contribution towards filling this gap.

Photo-curing of NOA65/E7 systems yields a rapid conversion with a transition from liquid like to rubbery or glassy materials.[22,23] Depending on the initial composition and the conditions of preparation, radical polymerization may produce heterogeneous networks consisting of dense and loosely cross-linked regions throughout the sample. These heterogeneities have profound impacts on thermophysical and mechanical properties of the films.

The precise knowledge of mechanical properties is important for an appropriate use of the polymer films as support media of high mechanical resistance and good electro-optic performance. Measurements of $T_g$ by DSC may not be reliable in the case of densely cross-linked networks and need to be validated by a thermomechanical analysis.

Undergoing stresses, materials like PDLCs usually show intermediate responses between solids and viscous media and their mechanical moduli are complex. The real part gives the elastic modulus while the imaginary part defines the loss modulus. In the present case, photo-curing of NOA65 systems yielded soft materials even in the absence of diluents like the low molecular weight liquid crystal E7. The knowledge of mechanical moduli led to important parameters such as the average molecular weight between cross-links which was a direct measure of the network cross-linking density. This parameter was needed to characterize the mechanical strength of the film and its thermophysical behavior since it appeared explicitly in the expression of the elastic free energy. Other viscoelastic parameters were also needed to complete the description of the rubber elasticity of the network but their determination relied on theoretical modeling that was beyond the scope of the present work.

## EXPERIMENTAL SECTION

### Materials and samples preparation

It was mentioned previously that the precise composition of Norland Optical Adhesive (NOA65) was protected by a commercial patent. However, it was reported in the literature that this compound was made essentially of four constituents[6,7,21]: trimethylolpropane diallyl ether, trimethylolpropane tris thiol, isophorome di isocyanate ester and benzophenone. The latter is a photoinitiator at a concentration of 5 wt %. The material used here was purchased from Thorlabs (Germany) and used without further modification. The curing by UV light generates radicals that start a chain of polymerization reactions according to the standard process. The glass transition temperature of the monomeric NOA65 was $-60^{\circ}$C. NOA65 had mercaptan dopants that were used for many adhesives with an excellent adhesion

and the ability to cure epoxies rapidly at ambient temperature. In addition, it had a very low toxicity compared to ordinary hardeners.

The LC E7 was purchased from Merck (Darmstadt, Germany). This eutectic mixture was made of 51 wt % 4-cyano-4′-pentyl-biphenyl (5CB), 25 wt % of 4-cyano-4′-heptylbiphenyl (7CB), 16 wt % of 4-cyano-4′-octyloxybiphenyl (8OCB), and 8 wt % of 4-cyano-4″-pentyl-p-terphenyl (5CB). It showed a glass transition at $T_g$(E7) = −60°C and a nematic to isotropic transition at $T_{NI}$ = 60°C with $\Delta H_{NI}$ = 4.61 $Jg^{-1}$.

Mixtures of NOA65 and E7 were prepared at different compositions and the photo-curing process was implemented using PIPS under UV exposure with a lamp Philips TL08 and a maximum absorption at the wavelength λ = 365 nm. The intensity used for full cure was 10 $mW/cm^2$ at this wavelength.

A drop of the initial formulation was put between two glass plates (rectangular micro-slides of 2.5 × 7.5 $cm^2$ commonly used for microscopy) to undergo exposure to the photo-curing source for a given period of time $t$. Films of about 100 μm thickness were elaborated and standard samples 4.4 mm wide and 20-mm long were prepared for the mechanical experiments.

## Experimental techniques

### Differential scanning calorimetry

An apparatus of type Mettler DSC 30 was used. Typically 10 mg of homogeneous NOA65/E7 mixtures were deposited on aluminum pans before curing and covered to perform the measurements. The thermal cycle applied in the measurements included a cooling ramp of 1°C/min allowing a precise identification of the temperature at the transition. A wide range of temperature (−100°C to +100°C) was scanned to explore the thermophysical behavior of photo-cured samples and detect major thermal events. At each composition, duplicate samples were considered to validate the results and the data analysis was based on averaged values.

### Polarized optical microscopy

Small amounts of NOA65/E7 mixtures were put on bare glasses on a stage under controlled atmosphere with nitrogen circulation. Samples were heated to bring the LC into the isotropic region above the NI transition temperature by nearly 15°C. A temperature control unit allowed to execute heating and cooling ramps. Recording of transition temperatures was made during a cooling ramp of 1°C/min. A video digital camera (CCD Hitachi KP-D50 color) linked to the microscope was used to visualize the selected morphologies under cross polarizers. The microscope was of type Zeiss (Germany) while the heating/cooling stage was a THMS 600 unit and the temperature control unit was a Linkham TMS 91 (Linkham Scientific Instruments, Water field, Surrey, UK).

### Mechanical spectroscopy

*Static measurements.* A mechanical testing machine Instron 6022 was used to perform static measurements. Rectangular samples of dimensions 20 × 4.4 × 0.1 $mm^3$ were cut in the parallel or perpendicular direction of the film and data were taken at room temperature (near 20°C) at a constant rate of 1 mm/min. Stress versus strain curves were obtained and Young's modulus was deduced from the slope of these curves. In each case, four duplicate samples were used to check the reproducibility of the results and the analysis was based upon averaged values.

*Dynamic measurements.* An apparatus of the type Rheometrics RMS 800 Mechanic Spectrometer was used for the Dynamic Mechanical Analysis under nitrogen atmosphere. Controlled deformation amplitude was changed with temperature from $10^{-4}$ at low temperature to $5 \times 10^{-2}$ at high temperature in the regime where linear viscoelasticity was applicable. Storage and loss moduli $E'$ and $E''$ were obtained for a given frequency as a function of temperature, LC concentration and curing time. Measurements were made in terms of the deformation frequency with a heating ramp of 2°C/min from −100°C ending at the temperature where the rubbery plateau was reached.

# RESULTS

## Thermophysical behavior

Figure 1 gives DSC thermograms of the photo-cured systems at several LC concentrations. The results showed distinct $T_g$s for the LC and the polymer matrix in addition to the nematic to isotropic transition temperature for the LC confined inside the randomly distributed droplets. $T_g$ of the cured polymer went up by 50°C reaching −10°C since $T_g$ of the uncured NOA65 was −60°C. On the other hand, the presence of small LC molecules induced a plasticizing effect by which $T_g$ of the polymer decreased almost linearly with the LC concentration reaching −20°C in the presence of 90 wt % E7. These features are illustrated in Figure 2 where both $T_g$s are shown in terms of the LC concentration. $T_g$ of the LC remained essentially constant meaning that it behaved as a pure component while confined in pores of the polymer matrix. The presence of two distinct $T_g$s for the

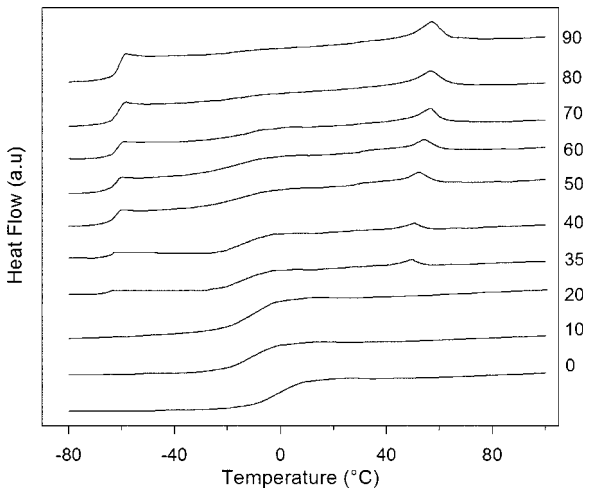


**Figure 1** DSC thermograms of the cured NOA65/E7 system for LC concentrations going from 0 to 90 wt % in the ascending order (numbers on the right hand side represent wt % E7).

LC and polymer was due to their reduced miscibility after the photo-curing process was completed.

Figure 3(a) features the phase diagram of the photo-cured system in the temperature versus LC concentration frame. This diagram was constructed on the basis of the DSC data and validated by optical microscopy observations as described in the experimental part. This procedure enhanced our confidence on the identification of the nematic to isotropic transition temperature. The solid line represents the calculated binodal according to the well documented theoretical method combining the Flory-Rehner free energy of rubber elasticity and the Maier-Saupe[7,15,24] free energy of nematic order. The computational method was exhaustively discussed in the literature and we skip this part referring the interested reader to the references cited above for the theoretical details. Interestingly, this diagram resembles that of the system reported in Ref. 25. Essentially three regions were identified with a different phase behavior. On the left hand side of the solid line, the system behaved as an isotropic liquid whereby E7 acted as an ordinary solvent. However, on the right hand side a large gap of miscibility emerged and a dense isotropic polymer phase coexisted with a pure phase made of the low molecular weight LC. Above 60°C, a liquid-like region described the phase behavior of the system but below 60°C, the pure LC phase showed a nematic order. The phase diagram of the initial uncured solution is shown in Figure 3(b) to illustrate the extend to which the phase behavior was changed due to cross-linking. While the miscibility gap in the initial mixture was limited to a narrow domain in the selected frame, that of the polymeric system extended to a much broader range of temperature and concentration. In the course of polymerization

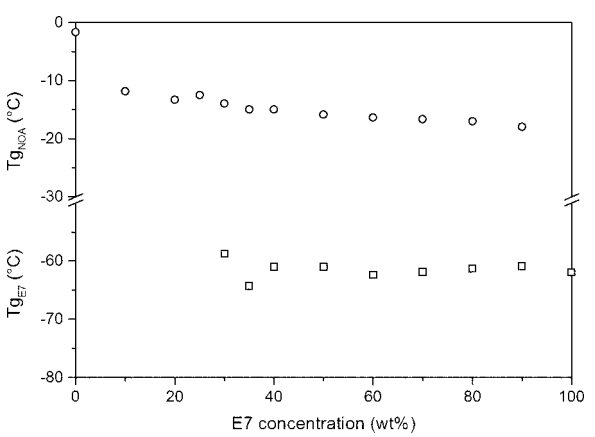


**Figure 2** Glass transition temperatures for the cured samples against the liquid crystal concentration. The upper curve gives $T_g$ of the polymer matrix while the lower curve shows that of the LC confined in droplets.

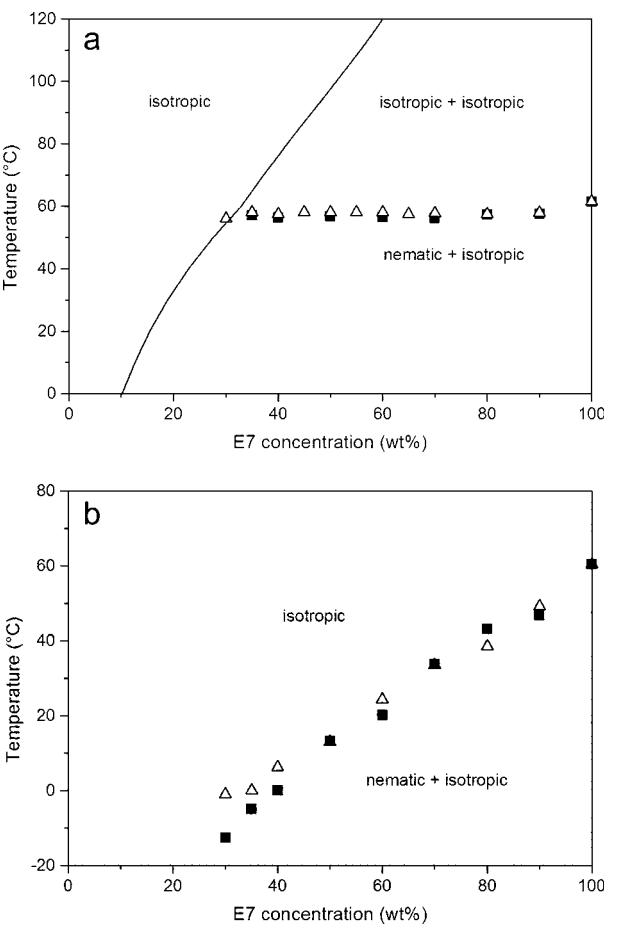


**Figure 3** (a) The phase diagram of the photo-cured NOA65/E7 system. Open triangles represent POM data (△) and the filled squares are DSC data (■). The solid line is the calculated curve. (b) The phase diagram of the uncured NOA65/E7 system. Open triangles represent POM data (△) and the filled squares are DSC data (■).

and cross-linking, the system underwent dramatic changes that were monitored in time by some thermomechanical measurements. While in Figure 3, the changes were expressed by displaying the phase diagrams in the initial and final states only, in the thermomechanical study, the analysis focused more on the time evolution of the system during the course of the photo-polymerization process.

### Static mechanical measurements

Uniaxial tests were performed by applying a stress to the films and measuring their deformations. The curves of the stress σ against strain ε are given in Figure 4, ε being the ratio of the actual sample length L to the initial length $L_0$ $\varepsilon = L/L_0$. The curves given in Figure 4(a) considered the effect of curing times on the pure NOA65 system. Longer lasting curing times led to higher doses of UV radiation absorbed by the samples, hence more densely cross-linked networks, and higher mechanical strengths. When the low molecular weight LC was added to the initial mixture, after curing the mechanical strength of the films weakened but the qualitative trends of the σ(ε) curves were preserved as indicated by Figure 4(b,c). We limited ourselves to 35 wt % LC simply because above this concentration, it became difficult to get appropriate films for mechanical testing experiments. The ultimate strain and breaking stress were quite low unless the system contained diluent but the tensile strength dropped abruptly with the diluent's concentration. A similar behavior was found by Olivier et al. in Ref. 26. From the initial slope of the curves in Figure 4, we were able to obtain Young's modulus under various conditions. The results are shown in Figure 5 where one could see that for pure NOA65, Young's modulus underwent a sharp increase in early stages but took more that 2 h to reach the saturation level. Adding diluent, the variation of Young's modulus versus time exhibited again the same fast initial increase followed by a saturation step within roughly 30 min. However, the modulus was found to drop significantly. The presence of a small amount of LC induced a significant plasticizing effect with a strong reduction in the film mechanical strength. By adding 35 wt % LC, Young's modulus dropped by a factor 4 compared to pure NOA65. The presence of small molecules led to much loosely cross-linked networks compared to pure monomeric systems.

Softening of the network due to excess LC was also illustrated in Figure 6 where Young's modulus was plotted against LC concentration. Nearly a factor 3 was found between the modulus of the network with 35 wt % E7 and that of pure NOA65. The sharp nonlinear decrease of the modulus with the LC content was consistent with the findings of

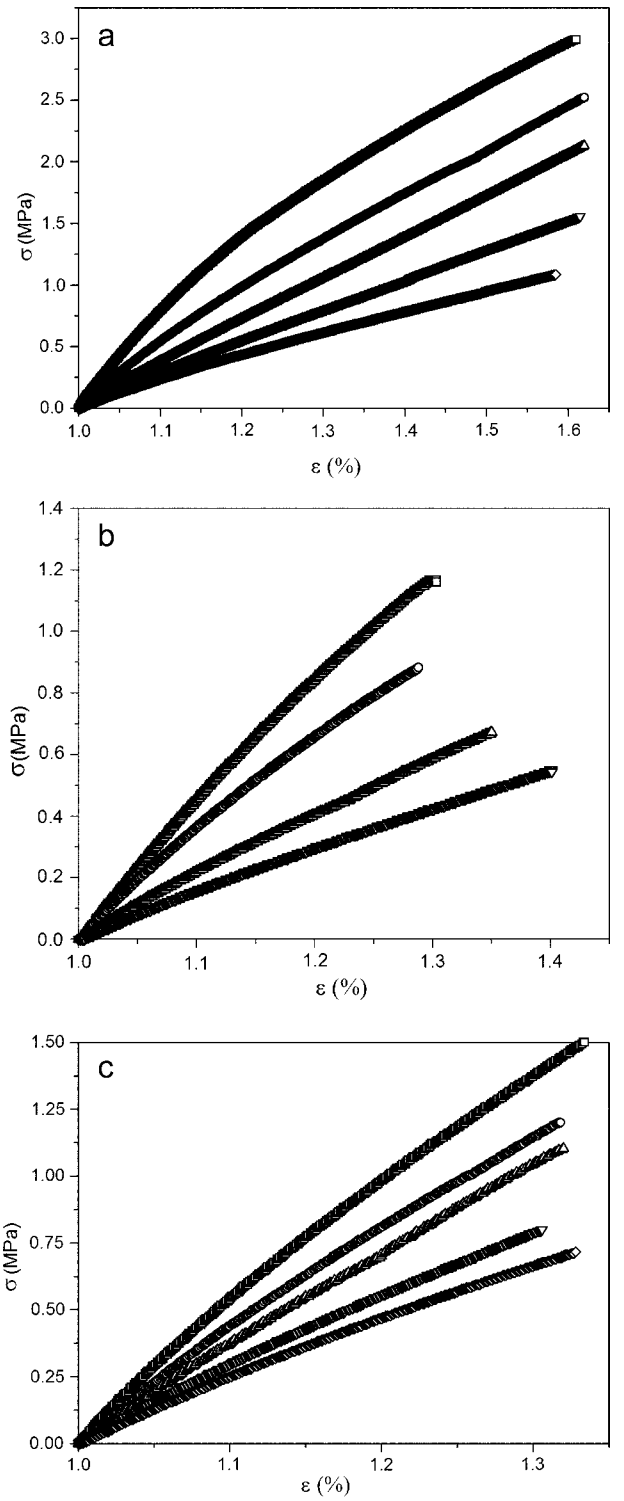


**Figure 4** Stress versus strain σ(ε) curves. (a) UV-cured pure NOA65 system at different times of exposure. The curves correspond in the descending order and in minutes to 60(□), 30(○), 20(△), 10(▽), 5(◇). (b) NOA65/E7 (15 wt % E7) system at different times of exposure. The curves correspond in the descending order and in minutes to 30(□), 20(○), 10(△), 5(▽). (c) NOA65/E7 system obtained during 20 min exposure. The curves correspond in the descending order and in (wt % E7) to 0(□), 20(○), 25(△), 30(▽), 35(◇).

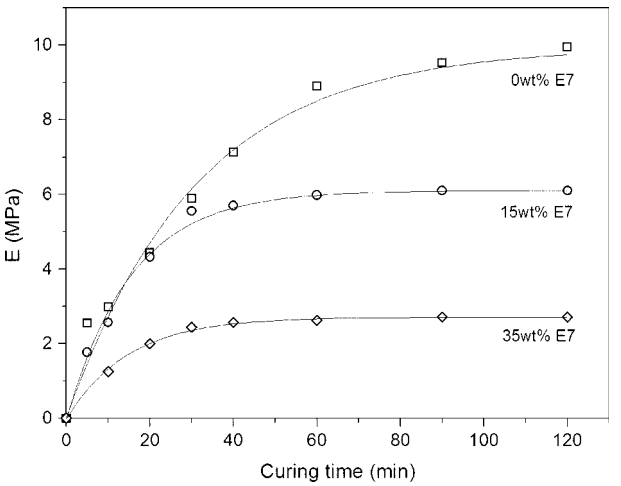


**Figure 5** Young's modulus $E$ (MPa) versus curing time. Upper curve pure NOA65 (□); Middle curve NOA65/E7 (○) with 15 wt % E7; Lower curve NOA65/E7 (◇) with 35 wt % E7. The solid lines are guides for the eye.

Ref. 26 for other systems and also in agreement with the dynamic data discussed below. To give more insight to the time evolution of the cross-linking density, the average molecular weight between cross-links $M_c$ is given in Figure 7 against curing time for different LC concentrations. The mass $M_c$ was a direct measure of the cross-linking density complementing that of Young's modulus $E$. These properties are related by $E = \frac{\rho RT}{M_c}$ where ρ is the mean density and $R$ the ideal gas constant.

Considering the fact that the exact composition of NOA65 was not known and using the information available in the literature, we could roughly estimate the molar mass of the monomeric unit of NOA65 as $M_0 = 400\,\mathrm{g/mole}$. Therefore, one could obtain the mean number of monomers between consecutive cross-links as $N_c = \frac{M_c}{M_0}$ which was an important parameter required to determine the elastic free energy of the network. Figure 7 shows that $M_c$ drops quickly with curing time as a direct consequence of the enhanced cross-linking density. A saturation limit was reached after nearly forty minutes of photo-curing. In the case of pure NOA65, the value $N_c = 4$ was attained after 30 min of UV exposure. These data suggested that the kinetics of cross-linking was slowed down rapidly as the initial mixture was further diluted with the LC E7.

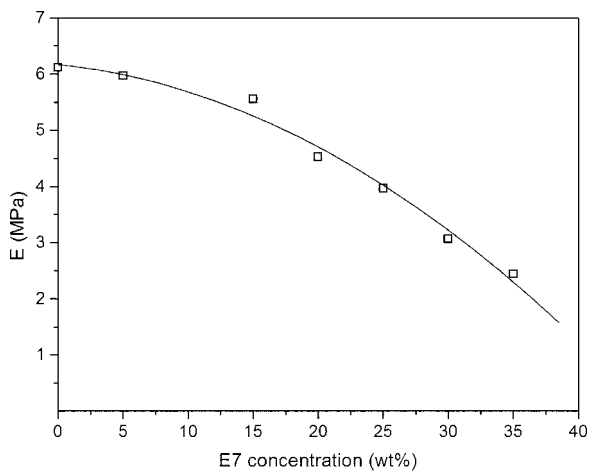


**Figure 6** Young's modulus $E$ (MPa) versus E7 concentration (wt%) for the NOA65/E7 system obtained during 30 min of curing time. The solid line is a guide for the eye.

## Dynamic mechanical analysis

A dynamical mechanical investigation was performed on the same systems. The response to a periodic stress with a given frequency was analyzed to deduce the elastic and loss moduli denoted E′ and $E''$, respectively. Recall that in the present case the mechanical response yielded a complex modulus with $E^* = E' + iE''$, where i represents the complex quantity $\sqrt{-1}$.

Figure 8 shows how the storage modulus $E'(T)$ curves evolved with curing time. Coming from the low temperature region with the system in the glassy state, the curves underwent a sharp drop at $T_g$ of the polymer. Below this temperature, there was no temperature dependence as one would expect from a system in the glassy state. The descent to the rubbery plateau was steeper for shorter curing times, which meant that the cross-linking process was not yet completed.

To complete the analysis of the dynamic data, the loss modulus $E''$ is shown in Figure 9 against temperature for different curing times. Consistent with the behavior of $E'$, $E''$ showed practically no sensitiv-

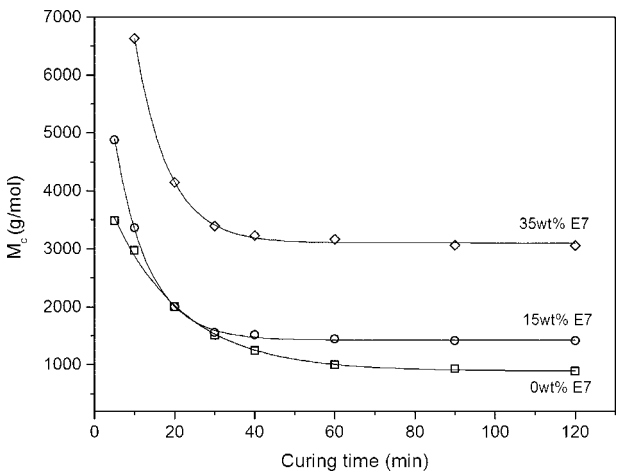


**Figure 7** The molecular weight between consecutive cross-links $M_c$ versus curing time and E7 concentration ($M_c = \frac{\rho RT}{E}$). Lower curve pure NOA65 (□); Middle curve NOA65/E7 (○) with 15 wt % E7; Upper curve NOA65/E7 (◇) with 35 wt % E7. The solid lines are guides for the eye.

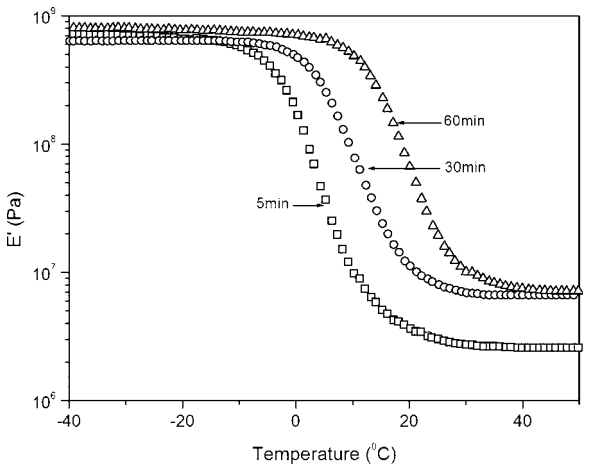


**Figure 8** Elastic storage modulus $E'$(Pa) versus temperature for pure NOA65 systems obtained at different curing times corresponding in the descending order to 60(△), 30(○) and 5(□) minutes (the frequency was fixed at 10 rad/s).

ity to the temperature below $T_g$ but exhibited a sudden drop after a maximum at the glass transition temperature $T_g$. In the glassy state, below $T_g$ all the curves merge together independent of the time of UV exposure. The corresponding curves for tangent of loss angle (i.e. $\tan\delta = \frac{E''}{E'}$) are given in Figure 10 also showing a maximum at $T_g$. Positions of these maxima were commonly taken as the glass transition temperatures from thermomechanical data. Figure 11 compares the results for $T_g$ with those of DSC thermograms. All the data showed a consistent steady increase of $T_g$ with time which was expected since the network cross-linking density was more enhanced with longer photo-curing periods. However DSC data underestimated $T_g$ by several degrees as compared to thermomechanical measurements.

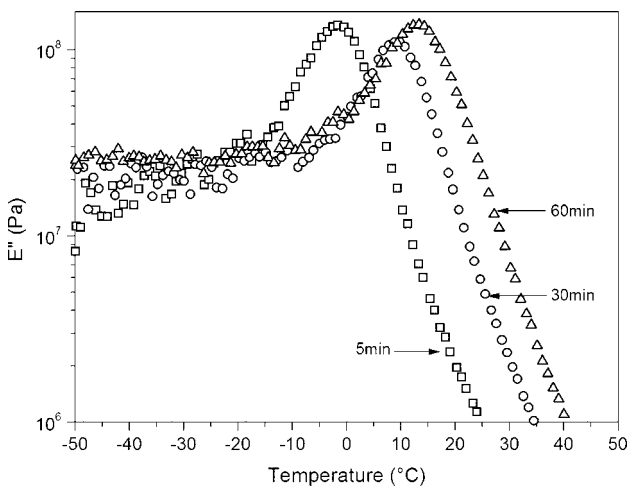


**Figure 9** Loss modulus $E''$(Pa) versus temperature for pure NOA65 systems obtained at different curing times: In the descending order, 60(△), 30(○), and 5(□) minutes.

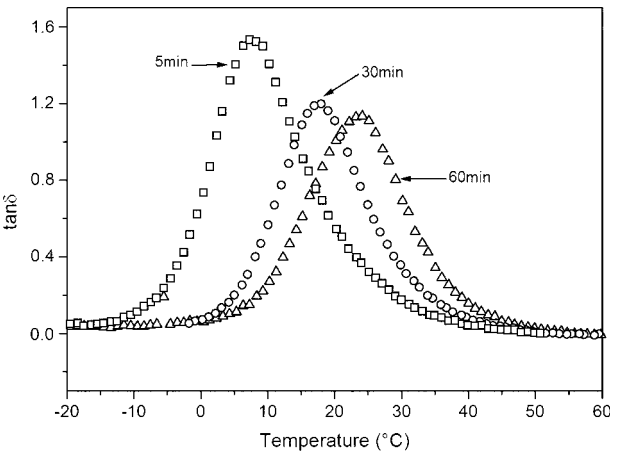


**Figure 10** Tangent loss angle (tan δ) versus temperature for pure NOA65 systems obtained at different curing times: From right to left, 60(△), 30(○) and 5(□) minutes.

These trends were also reported by Olivier et.al.[26] for other PDLC systems. Note that the discrepancy between DSC and thermomechanical data remained practically the same at all durations of the curing experiments.

## CONCLUSION

This article reported results of a combined investigation of thermophysical and thermomechanical properties of polymer and liquid crystal composite materials elaborated by polymerization induced phase separation and UV-curing. The initial mixture consisted of a thiol-ene formulation known as NOA65 and the eutectic mixture of low molecular weight liquid crystals E7. Thermophysical data showed dramatic changes in the characteristic transition temperatures after photo-curing. While the initial liquid showed a single $T_g$ at $-60^{\circ}$C, after photo-curing, two

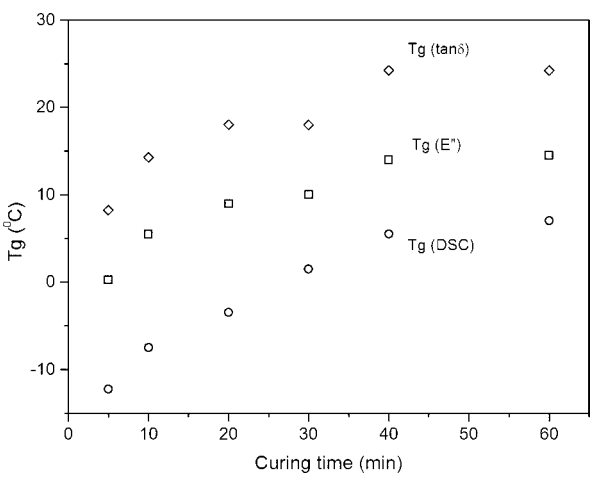


**Figure 11** $T_g$ versus curing time of pure NOA65 obtained from DSC (○), tan δ(◇) and the max of $E''$(□).

$T_g$s were observed: $T_g$ of the LC remained near $-60^\circ$C and that of the solid network jumped to $-10^\circ$C. Adding a low molecular weight liquid crystal to the polymer network induced a plasticizing effect which reduced $T_g$ of the polymer network almost linearly to $-20^\circ$C when the LC concentration approached 35 wt %. The phase diagram of the system underwent dramatic changes in the course of photo-curing and polymerization cross-linking processes. While the initial mixture retained the liquid morphology in a wide domain of temperature and composition with a narrow gap of miscibility at relatively high LC concentrations, the cured samples showed a very broad gap of miscibility both below and above the nematic to isotropic transition temperature. This is reminiscent of the important changes in the properties of the polymer dispersed liquid crystals in the course of the combined kinetics of the polymerization, cross-linking and phase separation. These changes are corroborated by the thermomechanical analysis performed using mechanical measurements both in the static and dynamic modes.

Thermomechanical properties changed dramatically during the cross-linking process of the compound. The system was initially liquid and as photocuring proceeded; it changed to a rubbery material with an increasingly high modulus. In the process of network formation, the increase of the mechanical modulus was of the order of $10^4$ or more. Some features were consistently determined in static and dynamic measurements corroborating the thermophysical results. A sharp descent of the elastic modulus with temperature at $T_g$ was validated by a maximum in the tangent of the loss modulus at the same temperature. This temperature was found to be systematically higher than in the DSC measurements for all systems investigated at different concentrations of the LC. Discrepancies in $T_g$ between DSC and mechanical data might be due to thermal hysteresis and scanning rates adopted in cooling and heating ramps but a comprehensive explanation of these discrepancies is still needed.

This article is dedicated to the memory of the late Professor Tadeuz Pakula in recognition for his constant encouragements and help. This work was accomplished while the first author (R. Benmouna) was a member of the International Max-Planck Research School at the Max-Planck Institute for Polymer Research (Mainz, Germany). He thanks Dr. R. Berger for enlightening discussions and Dr. Schiewe for encouragements.

## References

1. Drzaic, P. S.; Liquid Crystal Dispersions; World Scientific: Singapore, 1995.
2. Crawford, G. P.; Zumer, S. Liquid Crystals in Complex Geometries; Taylors & Francis: London, 1996.
3. Doane, J. W. Polymer Dispersed Liquid Crystals Displays; World Scientific: Singapore, 1990.
4. Doane, J. W. In Liquid Crystals: Applications and Uses; Bahadur, B., Ed.; World Scientific: River Edge, NJ, 1992.
5. Ong, HL. Optical Properties of Polymer Dispersed Liquid Crystals, Nonlinear Optical Properties of Liquid Crystals and Polymer Dispersed Liquid Crystals; World Scientific: Singapore, 1997.
6. Smith, G. W. Phys Rev Lett 1993, 70, 198.
7. Kyu, T.; Nwabunma, D. Macromolecules 2001, 34, 9172.
8. Maschke, U.; Coqueret, X.; Benmouna, M. Macromol Rapid Commun 2002, 23, 159.
9. Benmouna, R.; Rachet, V.; le Barny, P.; Feneyrou, P.; Maschke, U.; Coqueret, X. J Polym Eng 2006, 26, 499.
10. Benmouna, R.; Rachet, V.; le Barny, P.; Feneyrou, P.; Maschke, U.; Coqueret, X. J Polym Eng 2006, 26, 655.
11. Bella, S. D.; Luchetti, L.; Simoni, S. Mol Cryst Liq Cryst 1999, 330, 247.
12. Bella, S. D.; Luchetti, L.; Simoni, S. Mol Cryst Liq Cryst 1998, 320, 129.
13. Luchetta, D. E.; Luchetti, L.; Gobbi, F.; Simoni, S. Mol Cryst Liq Cryst 2001, 360, 93.
14. Sansone, M. J.; Khanarian, G.; Leslie, T. M.; Stilles, M.; Altman, J.; Elizondo, P. J Appl Phys 2001, 67, 4253.
15. Shen, C.; Kyu, T. J Chem Phys 1995, 103, 7471.
16. Nwabunma, D.; Kim, K. J.; Lin, Y.; Chien, L. C.; Kyu, T. Macromolecules 1998, 31, 6806.
17. Nwabunma, D.; Kyu, T. Macromolecules 1999, 32, 664.
18. Nwabunma, D.; Chiu, H. W.; Kyu, T. Macromolecules 2000, 33, 1416.
19. Lovinger, A. J.; Amundson, K. R.; Davis, D. Chem Mater 1994, 6, 1726.
20. Qian, T.; Kim, J. H.; Kumar, S.; Taylor, P. L. Phys Rev E 2000, 61, 4007.
21. Iguanero, B. P.; Perez, A. O.; Tapia, I. F. Opt Mater 2002, 20, 225.
22. Fouassier, J. P.; Rabek, J. F. Radiation Curing in Polymer Science and Technology; Elsevier Applied Science: London, 1993.
23. Pappas, S. P. UV Curing: Science and Technology; Technology Marketing Corporation: Stamford, Connecticut, USA, 1978.
24. Benmouna, F.; Coqueret, X.; Maschke, U.; Benmouna, M. Macromolecules 1998, 31, 4879.
25. Roussel, F.; Maschke, U.; Buisine, J. M.; Coqueret, X.; Benmouna, F. Mol Cryst Liq Cryst 2001, 365, 685.
26. Olivier, A.; Pakula, T.; Ewen, B.; Coqueret, X.; Benmouna, M.; Maschke, U. Macromol Mater Eng 2002, 287, 656.